Neuron, Vol. 14, 1019–1027, May, 1995, Copyright © 1995 by Cell Press

Kinetics of a Human Glutamate Transporter

Jacques I. Wadiche,* Jeffrey L. Arriza,*
Susan G. Amara,*† and Michael P. Kavanaugh*
*Vollum Institute
†Howard Hughes Medical Institute
Oregon Health Sciences University
Portland, Oregon 97201

Summary

Currents mediated by a glutamate transporter cloned from human motor cortex were measured in Xenopus oocytes. In the absence of glutamate, voltage jumps induced Na^+-dependent capacitive currents that were blocked by kainate, a competitive transport antagonist. The pre-steady-state currents can be described by an ordered binding model in which a voltage-dependent Na^+ binding is followed by a voltage-independent kainate binding. At −80 mV, two charges are translocated per molecule of glutamate, with a cycling time of approximately 70 ms, which is significantly slower than the predicted time course of synaptically released glutamate. The results suggest that glutamate diffusion and binding to transporters, rather than uptake, are likely to dominate the synaptic concentration decay kinetics.

Introduction

In the CNS, control of the extracellular concentration of the amino acid neurotransmitter L-glutamate is critical both because of its role in synaptic transmission and because of its excitotoxicity (for reviews, see Jonas and Spruston, 1994; Attwell et al., 1993). Concentrative uptake is mediated by transporters that serve to couple the electrochemical gradients of one or more cotransported inorganic ions to that of glutamate (Balcar and Johnston, 1972; Kanner and Sharon, 1978). Several members of a gene family encoding glutamate transporters have recently been cloned (Kanai and Hediger, 1992; Pines et al., 1992; Storck et al., 1992; Tanaka, 1993; Arriza et al., 1994). In addition to glutamate transporters, this gene family also includes a transporter for neutral amino acids (Arriza et al., 1993; Shafqat et al., 1993). Because substrate uptake by these proteins is electrogenic, with net positive charge accompanying each molecule of substrate translocated into the cell, transport can be measured in real time using voltage-clamp recording (Brew and Attwell, 1987; Schwartz and Tachibana, 1990; Eliasof and Werblin, 1993; Arriza et al., 1993, 1994; Klockner et al., 1993). Transporters for the neurotransmitter glutamate are widely distributed in the human CNS (Arriza et al., 1994). Although there is strong evidence that block of glutamate uptake in vivo leads to neuronal damage (Lucas and Newhouse, 1957; Olney and Sharpe, 1969; Olney et al., 1971), the role of transport in modulating kinetics of glutamatergic synaptic transmission is less clear (Hestrin et al., 1990; Sarantis et al., 1993; Mennerick and Zorumski, 1994; Barbour et al., 1994; Tong and Jahr, 1994). Evaluating whether the transporter may modulate excitatory glutamatergic transmission requires assessing a number of factors, including the affinity and kinetics of postsynaptic glutamate receptors (Jahr, 1994; Lester et al., 1990; Trussell et al., 1994), as well as the kinetics, density, and localization of the transporters.

Kinetic and mechanistic information about electrogenic transporters and ion pumps can be obtained through the use of voltage clamp to study pre-steady-state membrane transport currents (Läuger, 1991). A powerful approach to isolate such currents involves the use of selective antagonists (Nakao and Gadsby, 1986; Hilgemann et al., 1991; Parent et al., 1992a; Mager et al., 1993, 1994; Rakowski, 1993; Cammack et al., 1994). A number of glutamate analogs that antagonize its transport have been identified (Ferkany and Coyle, 1986; Bridges et al., 1991). The majority of these analogs act as competitive substrates for transport and thus induce inward currents under voltage clamp (Barbour et al., 1991; Kanai and Hediger, 1992; Arriza et al., 1994). An exception is the conformationally constrained glutamate analog L-kainate, which competitively antagonizes glutamate transport without itself being transported or inducing a steady-state current (Arriza et al., 1994). Three human excitatory amino acid transporters (EAAT1, EAAT2, and EAAT3) vary in their sensitivity to L-kainate, which potently blocks uptake mediated by EAAT2 (K_d = 17 μM), but not EAAT1 or EAAT3 (K_d > 1 mM; Arriza et al., 1994). The present study exploits the actions of L-kainate on EAAT2 to isolate pre-steady-state currents that provide kinetic information about the transporter.

Results

Voltage Dependence of Steady-State Transport Currents

Large inward currents are observed when L-glutamate is applied to voltage-clamped Xenopus oocytes several days after microinjection of cRNA transcribed from the human EAAT2 cDNA (Figure 1A). The voltage dependence of the steady-state transport current was examined by subtracting current records during a series of command voltage pulses in the absence of L-glutamate from corresponding currents in the presence of a saturating concentration (1 mM) of L-glutamate (Figure 1B). In a cyclic transport model, a sudden perturbation of membrane potential is predicted to lead to a redistribution of the system to a new steady state as a consequence of changes in the rate constants of the voltage-dependent state transitions. The relative magnitude of the instantaneous and noninstantaneous components of the change in current following a voltage jump will depend on the fraction of transporters in the state preceding the charge translocating state transition. The voltage jump would be expected to result in a quasi-instantaneous change in the transport current

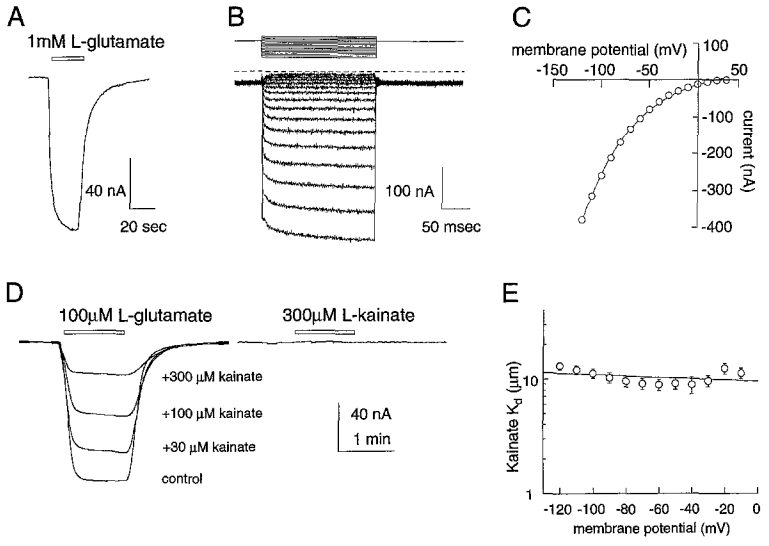

Figure 1. Voltage Dependence and Inhibition by L-Kainate of Steady-State L-Glutamate Transport Currents

(A) Inward current induced by bath application (indicated by bar) of 1 mM L-glutamate to a voltage-clamped oocyte expressing EAAT2. Holding potential, −60 mV.

(B) Voltage and time dependence of glutamate transport currents. Difference traces in a representative oocyte in response to 100 ms voltage pulses between +30 mV and −120 mV were obtained by subtraction of control currents from the corresponding currents in the presence of 1 mM L-glutamate. The dotted line represents I ≈ 0; holding potential, 0 mV.

(C) Steady-state current–voltage relationship from (B). The steady-state glutamate transport current increases e-fold per 55 mV.

(D) Bath application (indicated by bar) of 100 μM L-glutamate alone (control) and in the presence of varying concentrations of kainate in representative oocyte expressing EAAT2. Holding potential, −60 mV. Application of 300 μM kainate alone in the same oocyte does not induce a steady-state current.

(E) Voltage dependence of kainate K_d (mean ± SEM; n = 5) obtained from Schild analysis of inhibition of steady-state glutamate transport currents (see Arriza et al., 1994). Data were fitted by least squares to the equation $K_d = K_d^o \exp - (z\delta FV/RT)$ (Woodhull, 1973). The fit shown is for K_d^o = 9 μM and $z\delta$ = 0.03.

reflecting the time course of the voltage clamp, followed by a relaxation of the current with a time course reflecting the forward and backward rate constants of the state transitions through the cycle (Läuger, 1991). Similar to predictions of this model, the EAAT2 current relaxed to a new level following voltage jumps, with a time course exhibiting at least two exponential components, one with very fast kinetics ($\tau < 0.5$ ms; relative amplitude, 82%–86%), and a second with slower kinetics (τ = 10–30 ms; relative amplitude, 14%–18%; Figure 1B). The steady-state current increased exponentially with membrane hyperpolarization (e-fold per 55 ± 5 mV) and did not reverse at potentials up to +40 mV (Figure 1C).

Kainate Block of Steady-State Currents

The conformationally constrained analog of L-glutamate, L-kainate, selectively blocks transport currents mediated by EAAT2 without inducing a steady-state current itself (Figure 1D). The inhibition of EAAT2 transport by kainate is competitive with respect to glutamate (Arriza et al., 1994), suggesting that kainate binds to the external glutamate recognition site to form a nonproductive transport complex. To examine the voltage dependence of the kainate binding to the transporter, the glutamate dose shifts caused by coapplying various concentrations of L-kainate (10, 30, 100, and 300 μM) were measured at different membrane potentials. The kainate affinity determined by Schild analysis was relatively voltage independent, ranging from 10 to 14 μM (Figure 1E). The apparent fraction of the membrane electric field sensed by kainate was 3.4%, assuming a simple electrostatic ion binding model to a site on the transporter (Woodhull, 1973).

Kainate Actions on Transient Transporter Currents

In oocytes injected with EAAT2 cRNA, the capacitive transients resulting from voltage command pulses displayed a slower relaxation than water-injected oocytes. The mean time constant of relaxation for a 100 mV hyperpolarizing pulse was 506 ± 15 μs for oocytes expressing the EAAT2 transporter, compared with 144 ± 11 μs for water-injected oocytes when fits were constrained to one exponential (n = 6). To examine the possible existence of pre-steady-state charge movements mediated by the transporter, currents were measured during voltage jumps in the presence and absence of the antagonist L-kainate (Figure 2). In oocytes expressing the EAAT2 transporter, depolarizing voltage pulses from a holding potential of −40 mV to +60 mV showed that a component of the capacitive current was reduced in the presence of 300 μM kainate (Figure 2A, top). Subtraction of current records in the presence of kainate from those in control solution revealed a transient current that was outward upon depolarization and was followed by a transient inward current upon membrane repolarization (Figure 2A, bottom). In contrast, the capacitive and ionic currents of an uninjected oocyte that resulted from the same voltage jump were not affected by changing control solution to a solution containing the same concentration of L-kainate (Figure 2B). The kainate-sensitive transient current seen in oocytes expressing EAAT2 decayed within 10 ms following the voltage jump and did not exhibit any sustained steady-state component. Furthermore, the membrane conductance of oocytes expressing EAAT2 did not differ from matched control uninjected oocytes, suggesting that this transporter does not mediate a steady-state leak current, in contrast to some other glutamate transporters (Schwartz and Tachibana, 1990; Vandenberg et al., unpublished data).

Properties of Transient Transporter Currents

The charge movements induced by a jump from a given potential to various test potentials were calculated from the kainate-sensitive transient current–time integrals. Re-

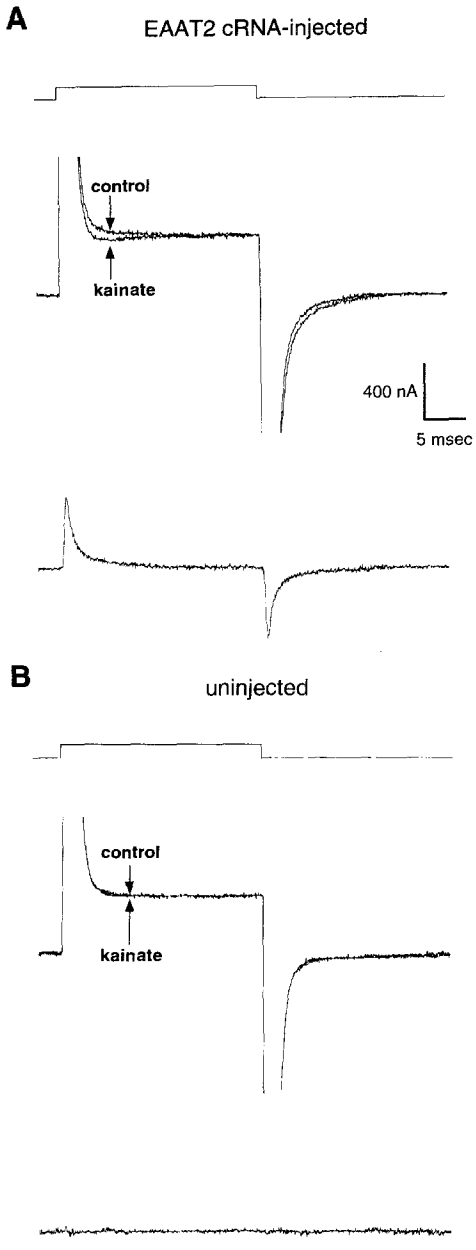

Figure 2. Kainate Blocks a Transporter-Specific Transient Current Induced by Voltage Jumps

(A) Currents recorded during 100 mV depolarizing voltage pulse in the presence of control (ND96) and 300 μM kainate solutions in a cell expressing EAAT2 (top). The oocyte was held at −20mV and stepped to +80mV for 25 ms, then repolarized back to −20 mV. Subtraction of current traces in kainate from control revealed a kainate-sensitive current that was outward in response to depolarizing pulses and inward upon the repolarization of the membrane (bottom).

(B) Same experimental treatments as (A) with an uninjected oocyte.

gardless of whether hyperpolarizing or depolarizing pulses were given, the charge movement during the test pulse was equal to the charge movement following the return to the original potential (Figures 3A and 3B). In addition, the conservation of charge movement was not affected by varying the duration of the voltage pulse (Figure 3C and 3D). These results strongly suggest that the kainate-sensitive transient currents are capacitive, resulting from a reversible charge movement rather than a resistive current flow through the transporter. The exponential time constant of the transient current relaxations exhibited a bell-shaped dependence on the pulse potential (Figure 3A). Fitting the relaxation time constants to a simple two-state model obeying a voltage-dependent equilibrium yielded a predicted charge movement (product of the charge valence and fraction of the field through which it moves; $z\delta$) of 0.46 for the state transition (Figure 3A).

The transient current–time integrals obeyed a Boltzmann function of membrane potential, with a midpoint of −3.2 ± 0.2 mV and slope factor of 61 ± 2 mV ($n = 19$; Figure 4A). This corresponds to a charge movement $z\delta$ of 0.41 ($RT/F \times 61$ mV), similar to that calculated from the voltage dependence of the relaxation time constants. As expected for a nonlinear saturable capacitance, the quantity of charge moved during a jump to a given potential depended on the prepulse potential, whereas the total charge movement (Q_{tot}), determined from fitting the charge movements over a range of potentials to the Boltzmann function, was independent of the prepulse potential. The average total charge movement blocked by 300 μM kainate in 19 cells was 2.57 ± 0.22 nC. Correcting for incomplete block by kainate at this concentration (see dose–response data below), the average Q_{tot} was 2.71 nC. The charge movement calculated from Boltzmann fits of individual cells was correlated with the transporter expression level as determined by the steady-state current induced by a saturating concentration (1 mM) of L-glutamate in the same cells (Figure 4B). Measurements of current–time integrals were made in various kainate concentrations and fitted to a Boltzmann function (Figure 5A). Kainate inhibited the charge movement in a saturable manner, with an EC_{50} of 16.9 ± 3.9 μM ($n = 4$) without significant effect on the voltage midpoint (Figure 5A and 5B). This EC_{50} value is also close to the K_d calculated from Schild analysis of inhibition of steady-state glutamate transport caused by kainate at different membrane potentials (10–14 μM; see Figure 1E). Taken together, these results suggest that the voltage-dependent transient current results from a nonlinear capacitive charge movement, which is inhibited by kainate binding to the transporter.

Ionic Basis of Transient Currents

The properties of the kainate-sensitive transient current demonstrate that it is capacitive. This current could result from a reversible conformational transition of the transporter (analogous to a gating current, involving movement of charged amino acid residues or polypeptide dipoles in the membrane field) and/or from binding and unbinding of an ion to a site within the membrane electric field. In Figure 6A, the kainate-sensitive transient current is seen in a representative cell that was subjected to 100 mV hyperpolarizing and depolarizing command pulses in normal recording medium containing 98.5 mM Na^+. The charge movements were abolished when external Na^+ was replaced by $Tris^+$ (Figure 6B). This result suggested the possibility that the transient current arises from a voltage-

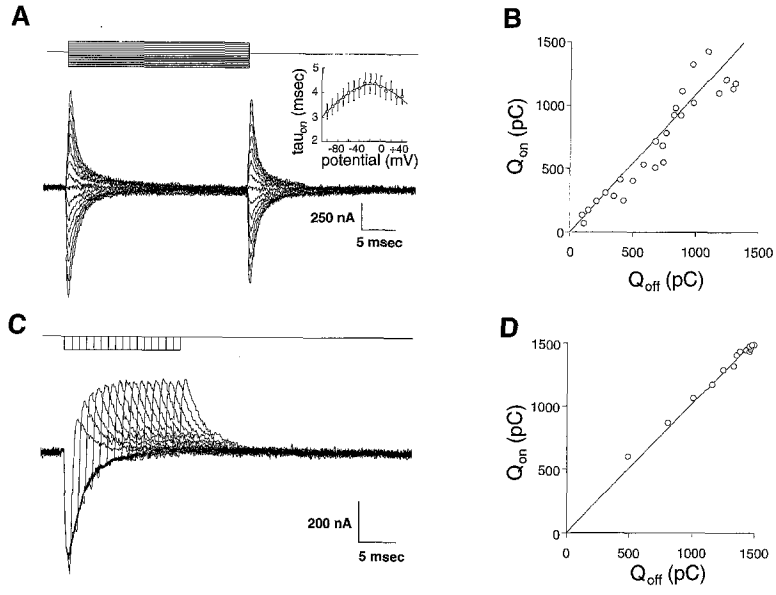

Figure 3. Pre-Steady-State Currents Blocked by Kainate Are Capacitive

(A) Family of subtracted current records in a representative oocyte showing voltage dependence of transient current blocked by 300 μM kainate. Difference currents were obtained as in Figure 3A. Voltage command pulses in 20 mV increments were 25 ms in duration from −160 to +120 mV from a holding potential of −20 mV. Inset shows voltage dependence of current relaxation time constants for hyperpolarizing command pulses from a holding potential of +50 mV to indicated test potentials (mean ± SEM; n = 5); data are fit to two-state model of charge movement (see Experimental Procedures) with an apparent valence of 0.46 and forward and backward rate constants at 0 mV of 136 s^{-1} and 98 s^{-1}, respectively.

(B) Correlation of kainate-sensitive charge movement during on and off pulses (from same cell as [A]) demonstrating conservation of charge movement. Line shows least squares fit; slope, 1.16.

(C) Time independence of conservation of kainate-sensitive charge movement. Envelope of difference currents recorded during a 100 mV hyperpolarizing voltage steps for 1–16 ms in 1 ms increments. Holding potential, −20 mV.

(D) Comparison of charge movement showing equality for incrementing on and off pulses from (C). Line shows least squares fit of data; slope, 0.97.

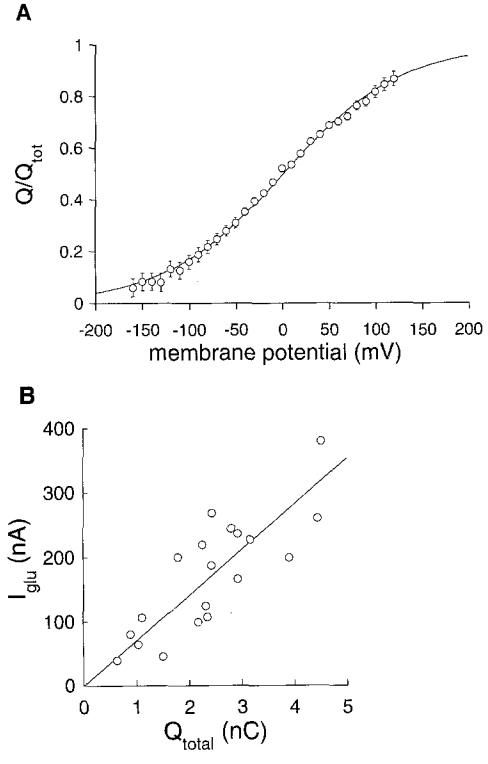

Figure 4. Voltage Dependence of Charge Movements Mediated by the EAAT2 Transporter

(A) Normalized charge movements (mean ± SEM; n = 19) from cells expressing the EAAT2 glutamate transporter were fitted by least squares to a Boltzmann function with $V_{0.5}$ = 3.2 ± 0.2 mV and slope factor 61 ± 2.4 mV (zδ = 0.41 ± .07). The charge movements in each oocyte were normalized to Q_{tot} in the same oocyte.

(B) Correlation of total charge movements with currents resulting from a saturating dose of L-glutamate (1 mM) at −80 mV for 19 oocytes, reflecting a range of transporter expression levels. Linear regression yielded a slope of 70 s^{-1}. The product of this slope and the effective valence of the charge movement (zδ = 0.41) equals the rate of steady-state charge transfer at this potential, 29 s^{-1}.

dependent binding and unbinding of Na^+ to a site on the external facing domain of the transporter, which is within the membrane electric field. Alternatively, Na^+ binding could enable a subsequent charge movement. The interaction of Na^+ with the transporter was further investigated by examining the effect of lowering $[Na^+]_{out}$ on the transient currents. Boltzmann analysis of the current–time integrals revealed that when $[Na^+]_{out}$ was reduced one-half by substitution with $Tris^+$, the total charge movement (Q_{tot}) remained the same, whereas the midpoint ($V_{0.5}$) was shifted −38 ± 5.5 mV (n = 6; Figure 6C). For the simple two-state model in which the charge movement results directly from Na^+ binding within the electric field (Figure 6D), then the shift in voltage midpoint can be used to calculate the effective fraction of the field, δ, sensed by Na^+ from

$$[Na^+]_1/[Na^+]_2 = \exp[\delta F(V_1 - V_2)/RT] \quad (1)$$

where $[Na^+]_1$ and $[Na^+]_2$ are the concentrations of Na^+ that half-saturate the transporter at membrane potentials V_1 and V_2, respectively. The −38 mV shift in the voltage midpoint would imply binding of a single sodium ion (or independent binding of multiple ions) to a site that traverses 46% ± 7% of the membrane electric field. In conjunction with the calculations of zδ from the independent measurement of the voltage dependence of charge movement (0.41; see Figure 4A) and transient current relaxation time constants (0.46; see Figure 3A), this result is consistent

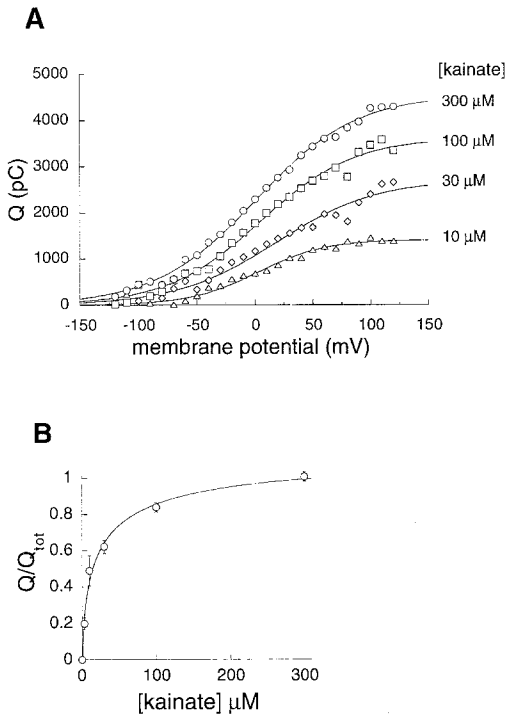

Figure 5. Kainate Concentration Dependence for Blockade of Charge Movements

(A) Boltzmann fits of charge movements blocked by varying kainate concentration in a representative cell.

(B) Kainate concentration dependence of normalized charge movement. Points (mean ± SEM; n = 4) were fitted by least squares to the expression $Q = Q_{tot}[kainate]/([kainate] + EC_{50})$, where Q is the total charge movement blocked by a given concentration of kainate as determined by fitting individual cells to a Boltzmann function as in (A). The EC_{50} for kainate block is 16.9 ± 3.9 μM.

with the simple model of charge movement arising from a single sodium ion binding (i.e., $z\delta = 1$) to a site on the transporter approximately 41%–46% of the distance through the membrane electric field, although more complex multistate models of charge movement are not ruled out by the data.

Determination of Transporter Density, Charge Stoichiometry, and Cycling Rate

In 19 oocytes, the average kainate-sensitive total charge movement (Q_{tot}) was 2.7 ± 0.2 nC, and the effective valence of the charge movement was 0.41 ± 01. These parameters can be used to determine N, the number of transporters, since

$$Q_{tot} = Ne_o z\delta \quad (2)$$

where e_o is the fundamental charge. The average number of transporters per oocyte was therefore 4.1×10^{10} (2.7×10^{-9} C/0.41 e_o). From capacitance measurements in the same cells, the oocyte membrane area was calculated to be $2.85 \times 10^7 \pm .14 \times 10^7$ μm², assuming a membrane capacitance of 10^{-6} F/cm². Thus, the average transporter density was 1439 μm^{-2}.

The charge flux through a single transporter can be determined from I_{ss}, the whole-cell steady-state current, and the number of transporters in the membrane. The number of elementary charges translocated per second by a transporter, ϕ, is given by

$$\phi = I_{ss}/(Ne_o) = I_{ss}/(Q_{tot}/z\delta) \quad (3)$$

Linear regression of the steady-state transport current in saturating glutamate at −80 mV versus Q_{tot} in oocytes expressing different numbers of transporters yielded a line with slope of 70 s^{-1}, which corresponds to a charge transfer rate of 29 s^{-1} (70 s^{-1} × 0.41; see Figure 4B). The voltage dependence of this rate was determined from measurement of the steady-state transport currents in saturating glutamate in the same group of oocytes. The steady-state charge transfer rate was increased by membrane hyperpolarization e-fold per 56 mV. The turnover rate of the transporter, which reflects the rate of glutamate translocation,

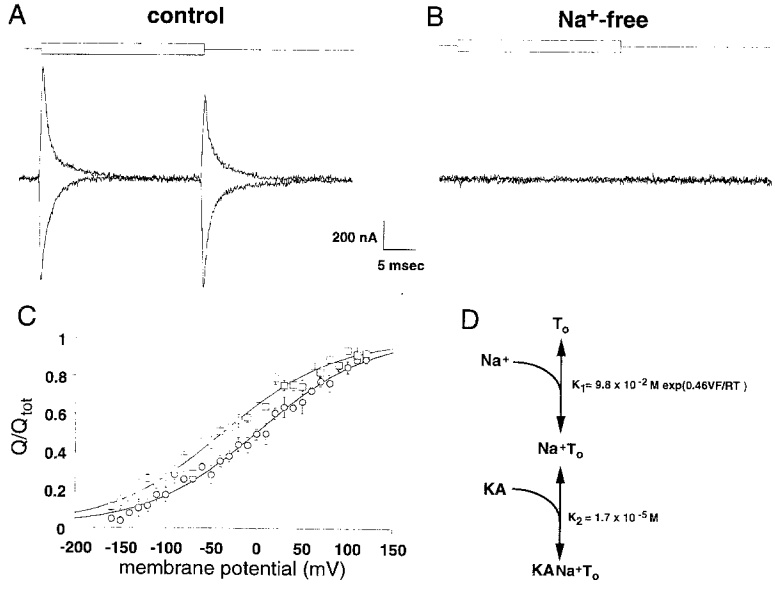

Figure 6. Na^+ Dependence of Charge Movements

(A and B) Kainate-sensitive transient currents resulting from 100 mV pulses of opposite polarity from a holding potential of −20 mV. Subtracted current traces in 98.5 mM Na^+ external solution (A) and Na^+-free buffer ($Tris^+$ substitution) (B).

(C) Normalized charge movements recorded in control recording medium (98.5 mM Na^+; circles) and 50 mM Na^+ (squares). Points represent mean ± SEM (n = 6). Data are fitted to a two-state model (shown in [D]) for a voltage-dependent binding of Na^+ to a site traversing 46% of the electric field, with a K_d at 0 mV of 98.5 mM (see Experimental Methods).

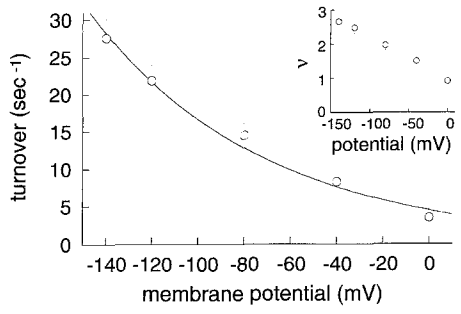

Figure 7. Voltage Dependence of Turnover Rate

Steady-state turnover, calculated from the ratio of the rate of translocation of charge per transporter at a given potential (obtained as in Figure 4B) divided by ν, the number of fundamental charges translocated per molecule of glutamate at the corresponding potential (inset; points represent mean ± SEM; n = 5–8). Data are fit to an exponential function showing an e-fold change in turnover per 76 mV.

is given by ϕ/ν, where ν is the number of charges translocated per cycle. To measure ν, current measurements were made during radiolabeled L-glutamate superfusion onto oocytes voltage clamped at potentials between 0 mV and −140 mV. The total quantity of charge translocated was calculated from the current–time integral during a 100 s pulse of 100 μM [^{3}H]L-glutamate, and the quantity of glutamate translocated was measured by scintillation counting. Normalizing the charge translocated per molecule of L-glutamate for 5–8 cells at membrane potentials between 0 mV and −140 mV gave a measure of the number of charges translocated per transport cycle, ν, which varied between 0.92 ± 0.15 and 2.66 ± 0.07 (n = 5–8; Figure 7, inset). Thus, at −80 mV, for example, the turnover rate $\tau = \phi/\nu = 29\ s^{-1} / 1.98 = 14.6\ s^{-1}$. Fitting the turnover rate to an exponential function of membrane potential revealed that it was increased by hyperpolarization e-fold per 76 mV (Figure 7).

Discussion

Analysis of nonlinear capacitance has been used extensively to obtain information about gating and kinetics of ion channels (for review, see Almers, 1978). This approach has also been applied to membrane transporters, in which qualitatively similar currents have been identified (Parent et al., 1992a, 1992b; Mager et al., 1993). The kainate-sensitive transient currents mediated by the human glutamate transporter EAAT2 have properties that suggest that they arise from a transporter-specific saturable capacitance due to Na^+ binding at a site on the transporter within the membrane electric field. These currents are distinguished by the following properties. First, the currents are blocked by the transporter antagonist kainate with the same concentration dependence as the block of steady-state transport. Second, the time integrals of the pre-steady-state currents for the forward and backward voltage jumps are equal. Third, the charge movement is well-fitted by a Boltzmann function of membrane potential. Fourth, the charge movements are abolished by removal of Na^+_{out}. Fifth, the voltage midpoint of the charge movement is shifted in a hyperpolarizing direction by reducing Na^+_{out} without changing the total charge movement.

The simplest model consistent with the observed actions of kainate involves a voltage-dependent binding of Na^+ followed by a voltage-independent binding of kainate to form a nontransported complex (see Figure 6D). In the absence of kainate, the free transporter is in voltage-dependent equilibrium with the Na^+–transporter complex. The equilibrium is perturbed by voltage jumps; hyperpolarizing voltage jumps induce charge movements due to Na^+ binding, whereas depolarizing voltage jumps induce Na^+ unbinding charge movements. In the presence of saturating concentrations of kainate, the charge movements no longer occur, because the equilibrium is driven towards the Na^+/kainate/transporter complex such that no further binding of Na^+ can occur following a hyperpolarizing voltage jump. The Na^+ binding site may be within the permeation pathway of the transporter, since the transporter appears to mediate directly flux of two Na^+ ions along with glutamate (Stallcup et al., 1979; Erecinska et al., 1983). Alternately, the Na^+ binding could occur at a site outside the electric field, which is then followed by a charge movement. In either case, the analysis of the voltage dependence of the equilibrium for the charge movement leads to the same estimate of transporter density and turnover. The average glutamate transporter density found in the present study (1439 μM^{-2}) is comparable to estimates for expression of the cloned γ-aminobutyric acid and 5-HT transporters in Xenopus oocytes (Mager et al., 1993, 1994), and is in addition consistent with estimates of [^{3}H]L-kainate binding site density (unpublished data).

At the present time, the precise stoichiometry of ions cotransported with glutamate is unknown. This stoichiometry will determine ν, the quantity of charge transferred per transport cycle. Direct measurements of ν at membrane potentials between 0 and −140 mV revealed that this quantity was voltage dependent, ranging from 0.9 to 2.7. This result differs from that predicted by a fixed model involving glutamate cotransport with two Na^+ ions and countertransport of one K^+ and one OH^- ion, leading to a net charge of 1 per cycle (Bouvier et al., 1992). This discrepancy appears to be due at least in part to a portion of the transporter current arising from a glutamate-activated chloride conductance that is not thermodynamically coupled to glutamate flux (Wadiche et al., 1995, Biophys. J., abstract). As a result, the number of charges translocated per molecule of glutamate varies with membrane potential, and the flux of amino acid through the transporter is less voltage dependent than the induced current. Whereas the glutamate-induced steady-state current varied e-fold per 55 mV (see Figure 1), the flux of amino acid varied e-fold per 76 mV (Figure 7). The rate of glutamate flux, which reflects the slowest forward rate constant in the transport cycle, varied from 4 s^{-1} to 27 s^{-1} over the voltage range 0 to −140 mV. Though the turnover is somewhat slower than the slow component of the glutamate current relaxation (see Figure 1B), the latter is expected to reflect forward and backward rate constants in the cycle (Läuger, 1991) and may be significantly faster than the rate-limiting forward rate constant (e.g., see Parent et al., 1992a, 1992b). The estimate

of glutamate turnover from the present study is significantly slower than estimates in retinal glial cells of salamander using different techniques ($>10^3$ s^{-1}; Schwartz and Tachibana, 1990) but is similar to estimates made with reconstituted glutamate transporters purified from rat brain (1.3 s^{-1}; Danbolt et al., 1990).

In principle, glutamate uptake may influence synaptic transmission by either altering the time course of clearance of synaptically released glutamate or by controlling the resting interstitial level of glutamate. Control of interstitial glutamate levels could modulate synaptic efficacy by tonic activation of receptors (Sah et al., 1989) or receptor desensitization (Trussell and Fischbach, 1989). Although γ-aminobutyric acid (Thompson and Gahwiler, 1992) and serotonin (Bruns et al., 1993) transporters can play central roles in shaping the time course of ionotropic receptor-mediated synaptic transmission, the influence of glutamate transport on the time course of ionotropic glutamatergic synaptic transmission is somewhat controversial (e.g., Isaacson and Nicoll, 1993; Sarantis et al., 1993; Mennerick and Zorumski, 1994; Barbour et al., 1994; Tong and Jahr, 1994). Glutamate receptor kinetics determine the time course of the postsynaptic response in hippocampal cultures (Lester et al., 1990; Colquhoun et al., 1992) with the decay time constant of glutamate in the cleft predicted to be very rapid, on the order of 1–2 ms (Clements et al., 1992; Colquhoun et al., 1992). A central question in studies of glutamatergic synaptic transmission relates to the relative roles of diffusion and reuptake in determining the time course of transmitter in the cleft. In support of a dominant role for diffusion, uptake blockers fail to alter the kinetics of synaptic currents in recordings from hippocampal slices (Hestrin et al., 1990; Isaacson and Nicoll, 1993; Sarantis et al., 1993). However, Barbour et al. (1994) found evidence for slowing of the time course of decay of postsynaptic currents by blockade of glutamate transporters in cerebellar Purkinje cells. Additionally, in cultured hippocampal neurons, Mennerick and Zorumski (1994) and Tong and Jahr (1994) reported changes in synaptic currents following transporter blockade consistent with alterations in transmitter clearance rate.

The present results suggest that the time constant for a complete cycle of transport at −80 mV is approximately 70 ms, significantly slower than the 1–2 ms time constant of glutamate decay estimated in hippocampal synapses (Clements et al., 1992; Colquhoun et al., 1992). This is still likely to be true at physiological temperatures, as the Q_{10} of the steady-state EAAT2 transport current is between 2.5 and 3 (unpublished data). However, a partial cycle of the transporter could occur on a much faster time scale than that of the entire cycle, which reflects only the slowest transition. Assuming a fast rate constant for glutamate binding, the transporters could speed the time course of glutamate decay by buffering free transmitter (Tong and Jahr, 1994). In this case, transporter density, which varies in different brain regions (Arriza et al., 1994; Rothstein et al., 1994), would be a factor in determining the concentration decay kinetics. In addition, synapse microanatomy will affect glutamate diffusion rates, and regional differences in this factor may contribute to variations in synaptic current kinetics (Barbour et al., 1994). The relatively slow transporter cycling time revealed by the present study suggests that glutamate transporter density and synaptic geometry, rather than reuptake, will be the dominant factors determining the kinetics of synaptic glutamate concentration decay.

Experimental Procedures

Transporter Expression and Electrophysiology

Capped cRNA transcribed from the human brain glutamate transporter EAAT2 cDNA (Arriza et al., 1994) was microinjected into Xenopus oocytes (50 ng per oocyte), and membrane currents were recorded 3–6 days later. Recording solutions (ND96) contained 96 mM NaCl, 2 mM KCl, 1 mM $MgCl_2$, 1.8 mM $CaCl_2$, and 5 mM HEPES (pH 7.4). In Na^+ substitution experiments, Na^+ was replaced with equimolar $Tris^+$. Two microelectrode voltage-clamp recordings were performed at 22°C with a GeneClamp 500 interfaced to an IBM compatible PC-AT using a Digidata 1200 A/D controlled using the pCLAMP program suite (version 6.0; Axon Instruments). Microelectrodes were filled with 3 M KCl solution and had resistances of less than 1 MΩ. For pre-steady-state current measurements, data were sampled at the lowest gain to avoid saturation of the amplifier response during the peak of the capacitance transient. Currents were low pass filtered at 1–2 kHz, digitized at 20 kHz, and signal-averaged six times before and after solution exchange. For measurements of charge movements, 25 ms command pulses in 10 mV increments from various holding potentials were made over a range from −160 mV to +120 mV before and after the application of kainate. Current traces in the presence of kainate were subtracted off-line from control currents. For each oocyte, the charge movements were calculated by time integration of the subtracted current records using Clampfit 6.0, then plotted versus voltage and fitted by least squares using Kaleidagraph v3.0 (Synergy Software) to the function

$$Q = Q_{tot}/(1 + \exp[e_o z\delta(V_m - V_{0.5})/kT]) + Q_{offset}$$

where Q_{tot} is the total charge movement, V_m is the membrane potential, $V_{0.5}$ is the midpoint of the charge movement, $z\delta$ is the product of the valence of the charge and apparent fraction of the field sensed by that charge, Q_{offset} is the offset that depended on the holding potential, e_o is the fundamental charge, k is the Boltzmann constant, and T is the absolute temperature. For comparisons among oocytes, charge movements were offset vertically by Q_{offset} and normalized to the Q_{tot} in the same oocytes. Time constants for relaxation of the transient currents were fitted to a two-state model with a symmetrical energy barrier in which charge movement occurs during forward or backward transitions with a time constant given by

$$\tau = 1/(\alpha^\circ \exp[z\delta e_o/2kT] + \beta^\circ \exp[-z\delta e_o/2kT])$$

where α° and β° are the forward and backward rate constants at 0 mV. A numerical simulation of the voltage and Na^+ concentration dependence of charge movements was developed using SCoP software (Simulation Resources, Berrien Springs, MI). Data were fit to a two-state model ($Na^+ + T \leftrightarrows TNa^+$) with a voltage-dependent dissociation constant $K = K^\circ \exp(z\delta FV/RT)$, where K° is the dissociation rate constant at 0 mV.

[^{3}H]L-Glutamate Flux

Voltage-clamp current recordings were made during superfusion of oocytes voltage clamped at indicated membrane potentials with 100 μM [^{3}H] L-glutamate (0.196 Ci/mmol; Amersham) for 100 s. Following washout, oocytes were rapidly transferred into a scintillation tube, lysed, and radioactivity was measured. Currents induced by [^{3}H]L-glutamate were recorded using Axotape software (Axon Instruments) and integrated off-line followed by correlation of charge transfer with radiolabel flux in individual oocytes.

Acknowledgments

This work was supported by National Institutes of Health grant

GM48709. We thank Scott Eliasof, Craig Jahr, Matt Jones, and Rob Vandenberg for helpful discussion and Weibin Zhang for Xenopus dissection and oocyte care. This work is in memory of Maurice Wadiche.

The costs of publication of this article were defrayed in part by the payment of page charges. This article must therefore be hereby marked *"advertisement"* in accordance with 18 USC Section 1734 solely to indicate this fact.

Received November 8, 1994; revised February 23, 1995.

References

Almers, W. (1978). Gating currents and charge movements in excitable membranes. Rev. Physiol. Biochem. Pharmacol. *82*, 96–190.

Arriza, J. L., Kavanaugh, M. P., Fairman, W. A., Wu, Y. N., Murdoch, G. H., North, R. A., and Amara, S. G. (1993). Cloning and expression of a human neutral amino acid transporter with structural similarity to the glutamate transporter gene family. J. Biol. Chem. *268*, 15329–15332.

Arriza, J. L., Fairman, W. A., Wadiche, J. I., Murdoch, G. H., Kavanaugh, M. P., and Amara, S. G. (1994). Functional comparisons of three glutamate transporter subtypes cloned from human motor cortex. J. Neurosci. *14*, 5559–5569.

Attwell, D., Barbour, B., and Szatkowski, M. (1993). Nonvesicular release of neurotransmitter. Neuron *11*, 401–407.

Balcar, V. J., and Johnston, G. A. (1972). Glutamate uptake by brain slices and its relation to the depolarization of neurones by acidic amino acids. J. Neurobiol. *3*, 295–301.

Barbour, B., Brew, H., and Attwell, D. (1991). Electrogenic uptake of glutamate and aspartate into glial cells isolated from the salamander (*Ambystoma*) retina. J. Physiol. *436*, 169–193.

Barbour, B., Keller, B. U., Llano, I., and Marty, A. (1994). Prolonged presence of glutamate during excitatory synaptic transmission to cerebellar Purkinje cells. Neuron *12*, 1331–1343.

Bouvier, M., Szatkowski, M., Amato, A., and Attwell, D. (1992). The glial cell glutamate uptake carrier countertransports pH-changing anions. Nature *360*, 471–474.

Brew, H., and Attwell, D. (1987). Electrogenic glutamate uptake is a major current carrier in the membrane of axolotl retinal glial cells. Nature *327*, 707–709.

Bridges, R. J., Stanley, M. S., Anderson, M. W., Cotman, C. W., and Chamberlin, A. R. (1991). Conformationally defined neurotransmitter analogues: selective inhibition of glutamate uptake by one pyrrolidine-2,4-dicarboxylate diastereomer. J. Med. Chem. *34*, 717–725.

Bruns, D., Engert, F., and Lux, H.-D. (1993). A fast activating presynaptic reuptake current during serotonergic transmission in identified neurons of Hirudo. Neuron *10*, 559–572.

Cammack, J. N., Rakhilin, S. V., and Schwartz, E. A. (1994). A GABA transporter operates asymmetrically and with variable stoichiometry. Neuron *13*, 949–960.

Clements, J. D., Lester, R. A. J., Tong, G., Jahr, C. E., and Westbrook, G. L. (1992). The time course of glutamate in the synaptic cleft. Science *258*, 1498–1501.

Colquhoun, D., Jonas, P., and Sakmann, B. (1992). Action of brief pulses of glutamate on AMPA/kainate receptors in patches from different neurones of rat hippocampal slices. J. Physiol. *458*, 261–287.

Danbolt, N. C., Pines, G., and Kanner, B. I. (1990). Purification and reconstitution of the sodium and potassium coupled glutamate transport protein from rat brain. Biochemistry *29*, 6734–6740.

Eliasof, S., and Werblin, F. (1993). Characterization of the glutamate transporter in retinal cones of the tiger salamander. J. Neurosci. *13*, 402–411.

Erecinska, M., Wantorsky, D., and Wilson, D. F. (1983). Aspartate transport in synaptosomes from rat brain. J. Biol. Chem. *258*, 9069–9077.

Ferkany, J., and Coyle, J. T. (1986). Heterogeneity of sodium-dependent excitatory amino acid uptake mechanisms in rat brain. J. Neurosci. Res. *16*, 491–503.

Hestrin, S., Sah, P., and Nicoll, R. A. (1990). Mechanisms generating the time course of dual component excitatory synaptic currents recorded in hippocampal slices. Neuron *5*, 247–253.

Hilgemann, D. W., Nicoll, D. A., and Philipson, K. D. (1991). Charge movement during Na^+ translocation by native and cloned cardiac Na^+/Ca^{++} exchanger. Nature *352*, 715–718.

Isaacson, J. S., and Nicoll, R. A. (1993). The uptake inhibitor L-trans-PDC enhances responses to glutamate but fails to alter the kinetics of excitatory synaptic currents in the hippocampus. J. Neurophys. *70*, 2187–2191.

Jahr, C. E. (1994). NMDA receptor kinetics and synaptic function. Sem. Neurosci. *6*, 81–86.

Jonas, P., and Spruston, N. (1994). Mechanisms shaping glutamate-mediated excitatory postsynaptic currents in the CNS. Curr. Opin. Neurbiol. *4*, 366–372

Kanai, Y., and Hediger, M. A. (1992). Primary structure and functional characterization of a high-affinity glutamate transporter. Nature *360*, 467–471.

Kanner, B. I., and Sharon, I. (1978). Active transport of L-glutamate by membrane vesicles isolated from rat brain. Biochemistry *17*, 3949–53.

Klockner, U., Storck, T., Conradt, M., and Stoffel, W. (1993). Electrogenic L-glutamate uptake in *Xenopus laevis* oocytes expressing a cloned rat brain L-glutamate/L-aspartate transporter (GLAST-1). J. of Biol. Chem. *268*, 14594–14596.

Läuger, P. (1991). Electrogenic Ion Pumps. (Sunderland, Massachusetts: Sinauer Associates).

Lester, R. A., Clements, J. D., Westbrook, G. L., and Jahr, C. E. (1990). Channel kinetics determine the time course of NMDA receptor-mediated synaptic currents. Nature *346*, 565–567.

Lucas, D. R., and Newhouse, J. P. (1957). The toxic effect of sodium L-glutamate on the inner layers of the retina. Arch. Opthalmol., *58*, 193–201.

Mager, S., Naeve, J., Quick, M., Labarca, C., Davidson, N., and Lester, H. A. (1993). Steady states, charge movements, and rates for a cloned GABA transporter expressed in Xenopus oocytes. Neuron *10*, 177–188.

Mager, S., Min, C., Henry, D. J., Chavkin, C., Hoffman, B. J., Davidson, N., and Lester, H. A. (1994). Conducting states of a mammalian serotonin transporter. Neuron *12*, 845–859.

Mennerick, S., and Zorumski, C. F. (1994). Glial contributions to excitatory neurotransmission in cultured hippocampal cells. Nature *368*, 59–62.

Nakao, M., and Gadsby, D. (1986). Voltage dependence of Na translocation by the Na/K pump. Nature *323*, 628–630.

Olney, J. W., and Sharpe, L. G. (1969). Brain lesions in an infant rhesus monkey treated with monosodium glutamate. Science *166*, 386–388.

Olney, J. W., Adamo, N. J., and Ratner, A. (1971). Monosodium glutamate effects. Science *172*, 294.

Parent, L., Supplisson, S., Loo, D. D., and Wright, E. M. (1992a). Electrogenic properties of the cloned Na^+/glucose cotransporter. I. Voltage-clamp studies. J. Membr. Biol. *125*, 49–62.

Parent, L., Supplisson, S., Loo, D. D., and Wright, E. M. (1992b). Electrogenic properties of the cloned Na^+/glucose cotransporter. II. A transport model under nonrapid equilibrium conditions. J. Membr. Biol. *125*, 63–79.

Pines, G., Danbolt, N. C., Bjoras, M., Zhang, Y., Bendahan, A., Eide, L., Koepsell, H., Storm-Mathisen, J., Seeberg, E., and Kanner, B. I. (1992). Cloning and expression of a rat brain L-glutamate transporter. Nature *360*, 464–467.

Rakowski, R. F. (1993). Charge movement by the Na/K pump in Xenopus oocytes. J. Gen. Physiol. *101*, 117–144.

Rothstein, J. D., Martin, L., Levey, A. I., Dykes-Hoberg, M., Jin, L., Wu, D., Nash, N., and Kuncl, R. W. (1994). Localization of neuronal and glial glutamate transporters. Neuron *13*, 713–725.

Sah, P., Hestrin, S., and Nicoll, R. A. (1989). Tonic activation of NMDA receptors by ambient glutamate enhances excitability of neurons. Science *246*, 815–818.

Sarantis, M., Ballerini, L., Miller, B., Silver, R. A., Edwards, M., and Attwell, D. (1993). Glutamate uptake from the synaptic cleft does not shape the decay of the non-NMDA component of the synaptic current. Neuron *11*, 541–549.

Schwartz, E. A., and Tachibana, M. (1990). Electrophysiology of glutamate and sodium co-transport in a glial cell of the salamander retina. J. Physiol. *426*, 43–80.

Shafqat, S., Tamarappoo, B. K., Kilberg, M. S., Puranam, R. S., McNamara, J. O., Guadano-Ferraz, A., and Fremeau, R. T., Jr. (1993). Cloning and expression of a novel Na^+-dependent neutral amino acid transporter structurally related to mammalian Na^+/glutamate cotransporters. J. Biol. Chem. *268*, 15351–15355.

Storck, T., Schulte, S., Hofmann, K., and Stoffel, W. (1992). Structure, expression and functional analysis of a Na^+-dependent glutamate/aspartate transporter from rat brain. Proc. Natl. Acad. Sci. USA *89*, 10955–10959.

Tanaka, K. (1993). Expression cloning of a rat glutamate transporter. Neurosci. Res. *16*, 149–153.

Thompson, S. M., and Gahwiler, B. H. (1992). Effects of the GABA uptake inhibitor Tiagabine on inhibitory synaptic potentials in rat hippocampal slice cultures. J. Neurophysiol. *67*, 1698–1701.

Tong, G., and Jahr, C. E. (1994). Block of glutamate transporters potentiates postsynaptic excitation. Neuron *13*, 1195–1203.

Trussell, L. O., and Fischbach, G. D. (1989). Glutamate receptor desensitization and its role in synaptic transmission. Neuron *3*, 209–218

Trussell, L. O., Raman, I. M., and Zhang, S. (1994). AMPA receptor kinetics and synaptic function. Sem. Neurosci. *6*, 71–79.

Woodhull, A. M. (1973). Ion blockage of sodium channels in nerve. J. Gen. Physiol. *61*, 687–708.